A NOVEL TECHNIQUE FOR MEASURING LOCAL BUBBLE SIZE DISTRIBUTION

Antonio Busciglio, Alberto Brucato, Francesca Scargiali and Franco Grisafi

Dipartimento di Ingegneria Chimica dei Processi e dei Materiali
Università degli Studi di Palermo,Dipartimento di Ingegneria Chimica dei Processi e dei material
Viale delle Scienze, Ed.6 – 90128 Palermo (Italy) –grisafi@dicpm.unipa.it

ABSTRACT: A novel experimental technique for measuring the local gas hold-up and the statistical distribution of local bubble size, is proposed. The technique is based on laser sheet illumination of the gas-liquid dispersion and synchronized camera, i.e. on equipment typically available in PIV set-ups. The liquid phase is made fluorescent by a suitable dye, and a band-pass optical filter is placed in front of the camera optics, in order to allow only fluoresced light to reach the camera CCD. In this way bubbles intercepted by the laser sheet are clearly identified thanks to the neat shade resulting in the images. This allows excluding from subsequent analysis all bubbles visible in the images but not actually intercepted by the laser sheet, so resulting in better spatial resolution and data reliability.
Preliminary data obtained in a stirred gas-liquid dispersion confirm the technique viability and reliability.

Keywords: gas-liquid systems, stirred vessels, image analysis, bubble size distribution

1. INTRODUCTION

Gas-liquid contactors are widely employed as reactors and bio-reactors in the process industry. Gas-liquid mass transfer is a common rate-determining step in these apparatuses. Local mass transfer areas depend on bubble size and concentration, and vary notably from place to place even in small stirred tanks (Calderbank [1958]; Sridhar and Potter [1980]; Barigou and Greaves [1992, 1996]). Mass transfer area is obtained most reliably from local gas hold-up and bubble size distribution (BSD). A thorough review of measuring techniques in gas liquid contactors can be found in Boyer et al. [2002].
Particle Image Velocimetry techniques (PIV) have been used in recent years for velocity field measurements in gas-liquid systems (Montante et al. [2007], Khopkar et al. [2003], Aubin et al. [2004]). One of the most innovative application of PIV setups is the measurement of BSD (Spicka et al. [2001], Liu et al. [2005]; Laakkonen et al. [2005]). As a matter of fact, PIV apparatuses, apart from providing information on the flow and turbulence quantities in gas-liquid systems, may be employed for other measurements, taking advantage of the possibility of isolating a well known volume of the systems. This, in conjunction with advanced Digital Image Processing Techniques can provide simultaneous measurements of both BSD and local gas hold-up.
In this work an advanced technique aimed at measuring the local gas hold-up and the statistical distribution of local bubble size, is proposed. The technique is based on laser sheet illumination and synchronized camera (i.e. on typical PIV equipment) in conjunction with a fluorescent liquid phase and a purposely developed image analysis procedure. Preliminary data obtained in a stirred gas-liquid dispersion are also presented and confirm the technique viability as well as its reliability.

2. EXPERIMENTAL SET-UP AND TECHNIQUE

The experimental system here investigated was a fully baffled cylindrical vessel (diameter T = 0.19 m) with a flat base, stirred by a standard six-bladed Rushton turbine (diameter D = T/3) offset by T/3 from vessel bottom. The liquid phase was deionised water in which a fluorescent dye (Rhodamine-B) had been dissolved. The gas phase (air) was supplied through a 6 mm ID open-ended pipe, centrally placed 10 mm below the turbine.

The gas-liquid dispersion was illuminated by a pulsed laser sheet (Nd-Yag, 50 mW per pulse, New Wave Research "Solo III", wavelength equal to 532nm). The resulting images were acquired by a digital high sensitivity 1280×1024 pixel (Hamamatsu) camera connected to a Dantec FlowMap 1500 synchronization/acquisition unit.

The cylindrical vessel was immersed in a water through in order to minimize optical distortions due to vessel geometry. A band-pass filter centred on the wavelength of fluoresced light (570nm) was placed in front of the camera in order to allow only this light to reach the CCD. On the basis of preliminary tests, an optimal Rhodamine concentration of 0.486 kg/m^3 was adopted. Higher concentrations result in too strong laser sheet attenuation, and therefore a troublesome non-uniformity in the tank illumination level, while lower concentrations give rise to excessively dark images. Gas flow rate of Q_g = 0.5 lt/min and at a rotational speed equal to 300 rpm were adopted for this work. The laser sheet .

3. IMAGE ANALYSIS TECHNIQUE

A typical image of the lower part of the vessel obtained by the above described apparatus is shown in Fig.1a, where the right border coincides with the vessel axis and the impeller region is digitally shielded in order to avoid spurious results in the subsequent image analysis. The laser sheet entered from the left side of the image and travelled towards the right side on a vertical plane at 45° between subsequent baffles. All the light observable in Fig.1a is that re-emitted by the fluorescent dye, that practically turns the laser sheet into a planar (fluoresced) light source.

In this image gas bubbles can be clearly observed. As it can be seen there are "dark bordered" bubbles, clearly placed beyond the light sheet, and "white bordered" bubbles. These may be either in front of the light plane or right on the light plane. These last are however easily identified as they are the only ones that give rise to a neat straight "shadow" in the image, caused by the fact that the laser light intercepted is diverted in many directions and fails to excite the dye on the light path rear the bubble. It may be worth noting that the vertical dark and white lines in Fig.1a is are baffle borders.
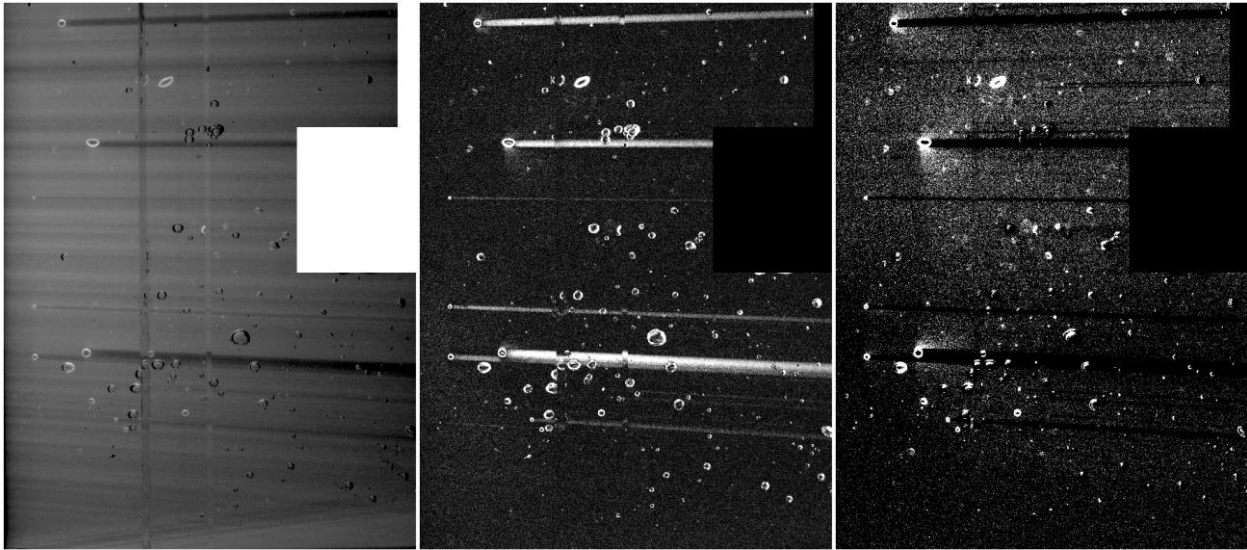

Fig. 1. From left to right, a) typical raw image of the vessel, b) absolute difference between raw and background images, c) simple difference between raw and background images.

Hence the imaging technique here proposed allows the unequivocal identification of the in-plane bubbles (those white-bordered and associated with the straight shadows) and, by discarding all other bubbles from subsequent analysis, the measurement of dispersion properties, such as gas hold-up and bubble size distribution, sharply pertaining to the investigated plane.

In order to improve the automatic recognition of the in-plane bubbles, some image processing is advisable, aimed at enhancing white borders and bubble "shadows".

The first processing step adopted in this work was background subtraction from the original image. It is worth noting that the average background luminance in the presence of gas bubbles was found to be quite different from that obtained in absence of gas, and lead to rather noisy images if adopted. Better results were obtained using time-averaged images of the gassed system as the background image. In this way, given the quite low gas flow rates investigated and correspondingly low gas hold-up, the noise introduced in the background image is of the order of 1% of the image signal.

Once a background image had been obtained it was subtracted pixel by pixel from the raw image. The resulting image is different depending on how the pixels with a resulting negative luminance are treated: they may be set to zero (hereafter referred to as "simple difference") or their absolute value may be considered ("absolute difference"). Notably:

- shadows have generally a luminance value smaller than the background image and the "absolute" difference, by exalting the darkest pixels, will make shadows very evident, as it can be seen in Fig. 1b. This last is therefore best suited for shadows identification;
- bubble white borders have a luminance value greater than the background image hence the simple difference between the raw image and the background will put them in evidence (Fig. 1c). Simple difference images are therefore best suited to exactly identify bubble size and position, once their in-plane position has been ascertained by the previous shadows elaboration.

Though not strictly needed, after trial and error attempts, improvement in bubble automatic identification was obtained by further image processing. In particular images like Figs 1b and 1c underwent 2-dimensional Wiener filtering (a pixelwise adaptive method based on statistics estimated from a local neighborhood of each pixel), "bottom-hat" filtering (aimed at making the back-noise of the image more uniform) and laplacian filtering (for border enhancing). All of these filters are available within the "MATLAB Image Tookit". The enhanced simple difference image resulting by applying the above filters to Fig.1c is shown in Figure 2.a, while the difference between the image resulting from Fig.1b after application of the above filters and the enhances simple difference (Fig.2a), is shown in Fig.2b. This last was found to be best suited image for subsequent automatic shadow identification.
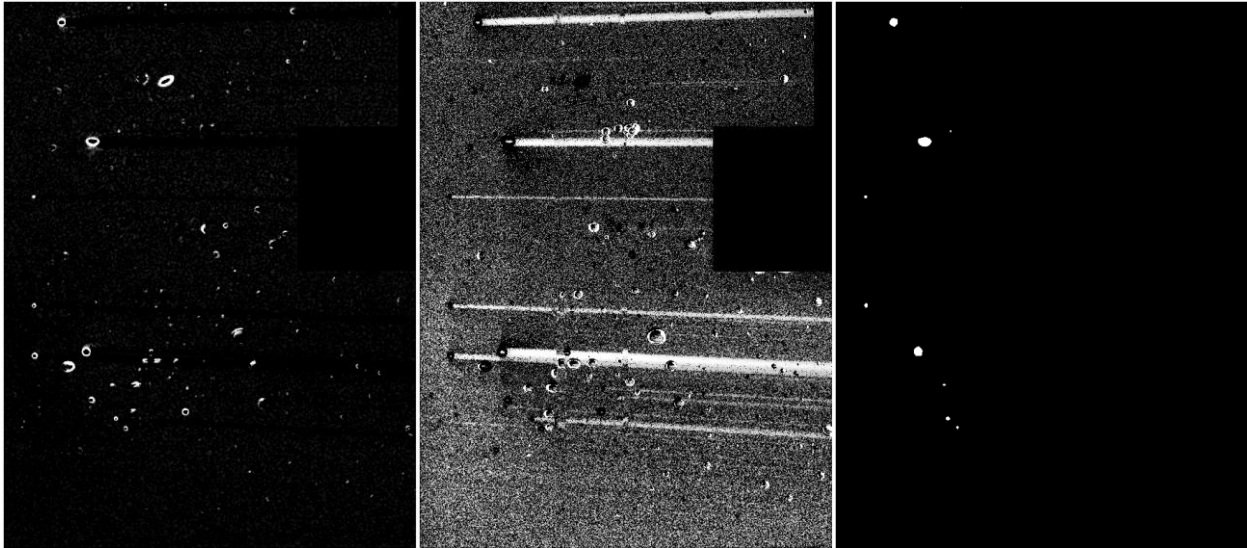

Fig. 2. From left to right, a) enhanced shadow image (enhanced "absolute" – enhanced "simple" differences), b) enhanced "simple" difference image, c) final binarized image of isolated in-plane bubbles.

For shadows automatic recognition in Figure 2.b no standard algorithms for straight lines recognition (for instance based on image Fourier transforms) could be employed, because of: i) the diffuse border of the shadows, ii) the non-uniform intensity of the shadows and iii) the fact that the shadows are not exactly parallel to each other. However, as the laser behaves as a pointwise source, bubble shadows concur to the same point, covering a certain angle range

with respect to the horizontal direction. Hence the shadow recognition algorithm employed was based on the only invariant property of the shadows themselves, i.e. the common passage through the laser emission point.

In particular, since the emission point and the range of angles (with respect to the horizontal plane) included in the image are known, it is possible to isolate only the pixel sequences lying on each possible laser ray. Each of these pixel sequences will behave differently whether it includes a shadow or not. Namely:
- the average value of pixel luminance will be greater when a bright shadow is involved, while a lower mean value will be observed in the other case;
- a linear fitting of the pixel sequence will show almost zero inclination only if no shadow is involved;
- a best fit with a sigmoidal function will show a sharp transition value of average pixel luminance, marking the presence of a bubble, only if a shadow is included;

As a consequence parameters like the average luminance, the slope and intercept of linear fit, or the values of best fitted parameters in the following sigmoidal function:

$$y = \frac{\alpha}{\exp(-\beta)+1} - \gamma \tag{1}$$

could be used for shadow identification. The resulting plots are shown in Fig.3 A-D, where the parameter values have been normalized in order to get a unit value for their maximum.
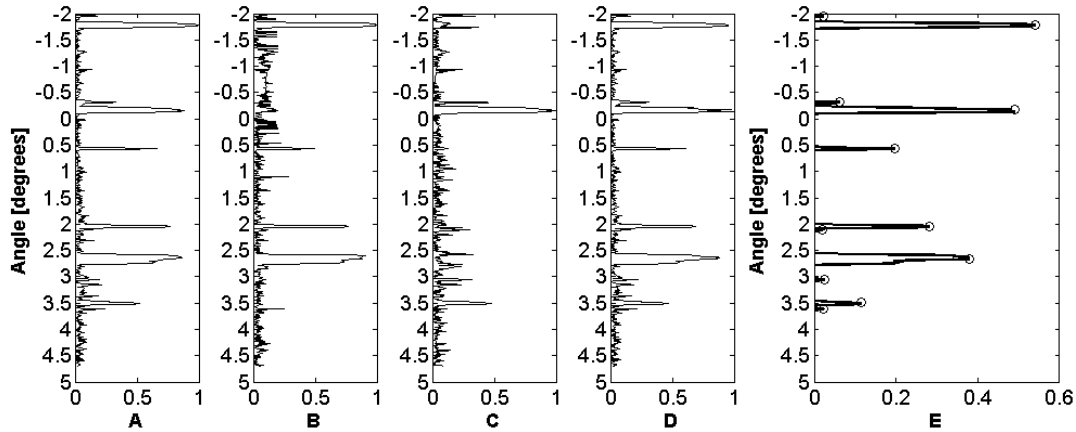

Fig. 3. Computed parameters: A) Intercept of "robust" linear fitting; B) Slope of robust linear fitting; C) Average luminance value; D) best fitted γ parameter of sigmoidal function (Eqn.1); E) Output function.

In practice none of the above parameters was found to be adequate on his own for a robust shadow recognition. Rather a suitable combination was employed in order to maximize reliability. This combination, referred to in the following as the "output function", was obtained by computing the square of the arithmetic average of the four normalized parameters. The result is shown in Fig. 3-E, where it can be seen that the output function is actually very effective in suppressing noise and making shadow identification very neat. The peaks, i.e. shadows (and in turn in-plane bubbles) automatically detected are marked with a circle in the same figure. The angle at which a peak is recognized is used to locate the bubble. The relevant peak width can be used for a first estimation of the bubble projected area for bubble isolation in the final image.

Once peak values of the output function have been identified, the pixel sequences pertaining to those angles are isolated and analyzed for bubble coordinates identification. The feature exploited to this end is that the cumulative sum of pixel sequences on a laser ray intercepting an in-plane bubble shows a characteristic linear trend, with a smaller inclination in the region before the bubble and a more pronounced inclination after the bubble, because of the greater value of pixel luminance (see Fig.2a). Hence, the point at which the inclination changes corresponds to the in-plane bubble position. Notably, the use of cumulative sums was found to enhance the algorithm robustness.

Identified bubbles are then "binarized" and "morphologically filled", in order to obtain, as final output, the binarized image shown in Figure 2.c. In this image, white pixels (luminance=1) represent pixels occupied by the gas phase while black pixels (luminance=0) are those occupied by the liquid phase. For each bubble present in the image, its area, equivalent diameter and centroid coordinates can be computed and stored, and so allowing the reconstruction of local as well as overall bubble size distributions.

Notably, the average pixel luminance over time obtained by superposition of many binarized images, clearly gives the local probability of gas phase occupation in each pixel. Such probability practically coincides with local gas hold up. The technique is therefore able to result into neat local gas hold-up maps, with reasonable effort and without any intrusion in the system.

3. PRELIMINARY RESULTS

The procedure viability was checked by processing 2000 images obtained with the previously described experimental apparatus. It may be worth noting that collecting the 2000 images involved only few minutes of experimentation while much longer times were needed for the subsequent image processing. As a matter of fact, though with an un-optimized MATLAB procedure, about one CPU day was required on a Core 2 duo running at 2.33 GHz. It may be worth noting that for this type of computation parallelization is very easily accomplished by simply subdividing the total number of images to be processed among different jobs running on each available CPU.

Some of the results so obtained are shown in Figs 4a and b for bubble size distribution (BSD) and gas hold up respectively. I may be noted that, although the technique can in principle provide very detailed local bubble distribution information, 2000 images were sufficient to obtain statistically significant BSD information only over fairly large vessel macro-areas. It is for this reason, as well as for space limitations, that only vessel averaged BSD is given here in Fig.4a, where it can be observed a characteristically skewed BSD. From this the main distribution moments ($D_{10} = 1.14$ mm, $D_{32} = 2.49$ mm, $D_{43} = 3.39$ mm) could easily be derived.

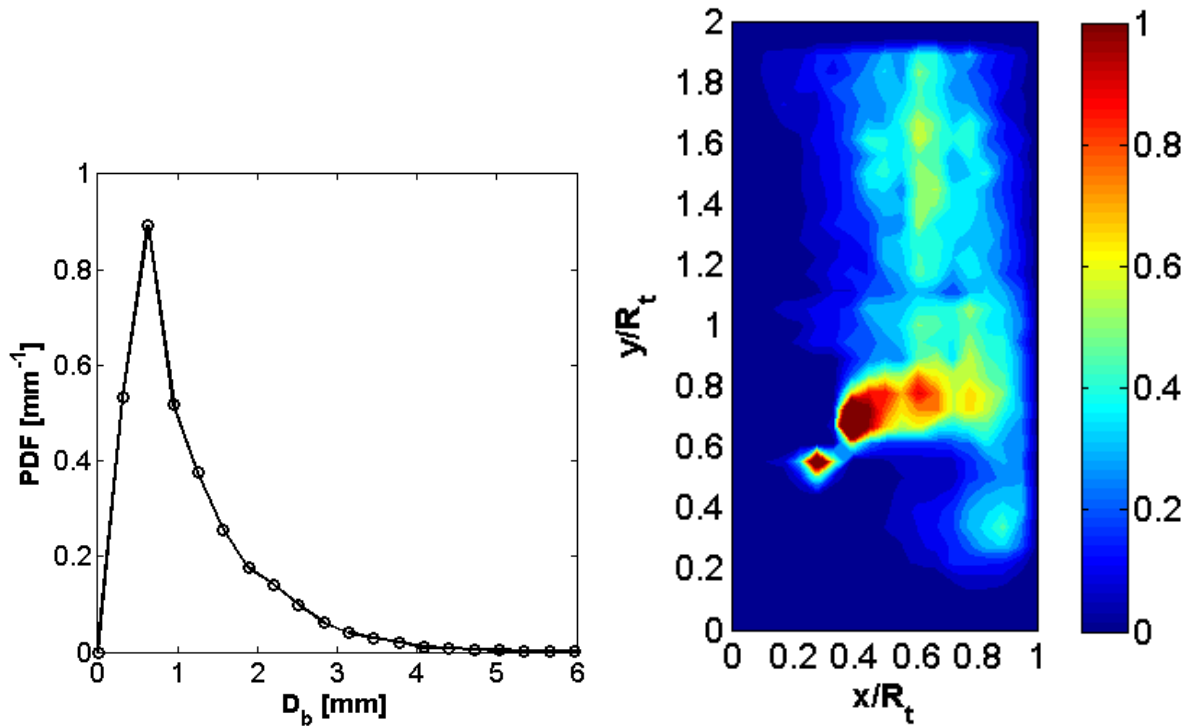

Fig. 4.   a) Bubble Size Distribution in the whole vessel
b) gs hold-up distribution map ($Q_g = 0.5$ lt/min, 300 rpm).

As it concerns gas hold-up, although in principle an extremely detailed information can be collected (an average hold-up datum in each of the 1280*1024 pixel locations) once again the 2000 images analysed were insufficient for getting statistically stable results and some data merging was needed to obtain meaningful results. The macro-areas needed for this purpose were (not surprisingly) found to be smaller than for BSD. In particular by merging results obtained over 50*50 pixel areas the local gas hold-map map shown in Fig.4b was obtained.

As it can be seen, the map is qualitatively consistent with experimental results by Barigou and Greaves (1996) as well as with expectations. If the time averaged gas hold up of Fig.4b is further averaged over the entire plane under investigation, a value of 0.22 % is obtained. Clearly in order to get a more rigorous comparison with volume averaged data, the entire procedure should be repeated over several vertical planes placed at different angles with repect to baffles should have to be considered. If the above hold-up and D_{32} results are accepted as being representative of the entire vessel volume, an interfacial area of $a_i = 6\,\varepsilon_g\,/D_{32} = 5.6$ m^{-1} can be computed. Notably, the relevant values predicted on the basis of well known literature correlations (Calderbank, 1958; Miller, 1975) are 0.26% and 5.5 m^{-1} for gas hold-up and interfacial area respectively. The excellent agreement found may be regarded as a validation of the novel technique here proposed.

4. CONCLUSIONS

A novel technique has been developed for measuring local bubble properties in gas liquid contactors. The technique is based on the use of a fluorescent liquid phase coupled with a laser sheet and a purposely developed digital image analysis routine. It may be regarded as being particularly reliable thanks to its ability to discard from the analysis all out of plane bubbles. It can be conveniently employed for measuring local features of gas liquid dispersions, such as bubble size distribution and gas hold-up, provided that sufficiently dilute dispersions are investigated. The technique viability was tested in the case of a gas-liquid stirred tank. The preliminary results obtained were found to be in very good agreement with expectations.

5. REFERENCES

Aubin J., Le Sauze N., Bertrand J., Fletcher D.F., and Xuereb C. (2004). PIV measurements of flow in an aerated tank stirred by a down- and an up-pumping axial flow impeller. Experimental Thermal and Fluid Science, 28:447–456,.

Barigou M. and Greaves M. (1992). Bubbles size distributions in a mechanically agitated gas-liquid contactor. Chem. Eng. Sci., 47(8):2009–2025,.

Barigou M. and Greaves M. , (1996). Gas holdup and interfacial area distributions in a mechanically agitated gas-liquid contactor. Chem. Eng. Res. Des., 74:397–405.

Boyer C., Duquenne A.M., and Wild G. , (2002). Measuring techniques in gas-liquid and gas-liquid-solid reactors. Chem. Eng. Sci., 57:3185–3215.

Calderbank P.H. , (1958). Physical rate processes in industrial fermentation. Part 1. the interfacial area in gas-liquid contacting with mechanical agitation. Trans. Inst. Chem. Engrs., 36:443–463.

Khopkar A.R., Aubin J., Xuereb C., Le Sauze N., Bertrand J., and Ranade V.V., (2003). Gas-liquid flow generated by pitched-blade turbine: particle image velocimetry measurements and computational fluid dynamics simulations. Ind. Eng. Chem. Res., 42:5318–533,.

Laakkonen M., Honkanen M., Saarenrinn P., and Aittamaa J. , (2005). Local bubble size distributions, gas-liquid interfacial areas and gas holdups in a stirred vessel with particle image velocimetry. Chemical Engineering Journal, 109:37–47.

Liu Z., Zheng Y., Jia L., and Zhang Q. (2005) Study of bubble induced flow structure using PIV. Chemical Engineering Science, 60:3537–3552.

Miller D.N. (1974), "Scale-up of agitated vessels gas-liquid mass transfer ", AIChE Journal, 20, 445-453.

Montante G., Magelli F., and Paglianti A. (2007). Experimental analysis and computational modelling of gas-liquid stirred vessels. IChemE, 85(A5):647–653.

Spicka P., Dias M.M., and Lopes J.S.B. , (2001). Gas liquid flow in a 2D column: Comparison between experimental data and CFD modelling. Chem. Eng. Sci., 56:6367–6383.

Sridhar P. and Potter O.E., (1980). Interfacial areas in gas-liquid stirred vessels. Chem. Eng. Sci., 35(3):683–695